Pergamon

Cement and Concrete Research 29 (1999) 339–347

CEMENT AND CONCRETE RESEARCH

Isothermal moisture properties of wood-cementitious composites

A. Bouguerra [a], H. Sallée [b], F. de Barquin [c], R. M. Dheilly [d], M. Quéneudec [d,]*

[a]*Université de Rennes 1, IUT de Rennes 1, B.P. 1144, 3, rue du Clos Courtel, 35014 Rennes Cédex, France*
[b]*CSTB de Grenoble, 24 rue Joseph Fourier, 38400 St. Martin d'Hères, France*
[c]*Centre Scientifique et Technique de la Construction, Division Matériaux, Avenue Pierre Holoffe 21, 1342 Limelette, Belgium*
[d]*Laboratoire Bâtiment: Université de Picardie Jules Verne, IUT, Département Génie Civil, Avenue des Facultés, Le Bailly, 80025 Amiens Cédex 01, France*

Manuscript received 27 May 1998; accepted manuscript 19 November 1998

Abstract

This article describes a study undertaken to examine the moisture properties of lightweight concrete prepared from clay, cement, and wood aggregates at isothermal conditions. The sorption-desorption isotherm curves of different mixtures show a strong hysteresis. The effect of wood aggregates on the water absorption of composite has been investigated by gamma ray absorption spectrometer. It is found that the sorptivity of the composite is very affected by the presence of wood aggregates in clay-cement matrix. Test results have been confirmed both qualitatively, using magnetic resonance imaging method, and quantitatively, from capillary suction curve calculated from sorption isotherm and pore size distribution.

Keywords: Moisture properties; Wood composites; Adsorption capillary

Building materials are all porous to a greater or lesser extent. Upon contact with an ambient environment that exhibits continually changing temperature and humidity, they show susceptibility both to the entrapment of water and, consequently, to the changes in their thermal and mechanical properties [1,2].

From the standpoint of hygroscopy, the absorption of water by a porous material starts with the physical adsorption of water vapour due to van der Waals forces. The various stages of adsorption have been previously described [3,4]. The first stage is the monomolecular adsorption phase, in which a single layer of water molecules covers the pores' surfaces and forms a physical bond with the pores. This only occurs for low values of relative humidity, and the adsorption speed is proportional to both the relative humidity and the free pore surfaces. The second stage is a polymolecular adsorption phase. A water film appears on the pore surfaces due to the adsorption of several layers of water molecules. This framework has already served as the basis for several theories [5–8].

However, such theories are only applicable for weak to moderate levels of relative humidity. For high relative humidity, liquid bridges can appear between the pore wall; this is known as the capillary condensation phase. According to this phenomenon, the narrow pores, known as condensable pores, fill up. A limit in the size of the pore radius, which corresponds to the critical water content, would appear to exist. According to Feldman et al. [9], this critical radius is considered to be $r < 100$ nm. Such a finding allows us to distinguish hygroscopic materials (wood and mortar) from those in which the quantity of water adsorbed by physical adsorption processes is relatively high compared both to the saturation threshold and to nonhygroscopic materials. With respect to the latter, the quantity of adsorbed water due to physical adsorption when the relative humidity reaches 99.9% is very low in comparison with the total volume accessible to water. The saturation threshold, S (the total volume accessible to water), can be expressed as the relation $S = \theta_v/\varepsilon$, where θ_v is the volumic water content, ε the total porosity, and $0 < S < 1$. To fill those pores with radii greater than the critical radius, it is necessary that the pores come into direct contact with liquid water. We therefore turn our attention to capillarity and define a capillary pressure P_c for the cylindrical pores being considered with a radius of r. Let $P_c = 2\sigma/r$, where σ is the air/water surface tension. This relation supposes a zero angle of contact between water/solid, which implies that the water completely fills the solid. The capillary suction ψ can then be expressed in terms of the water content in the considered pores, which in turn can be written in terms of the height of the water column and thus defined by the relation: $\psi = -P_c/\rho_e.g$, where ρ_e is the volumic mass of water and g is the gravitational

---

* Corresponding author. Tel.: 33-32253-4016; Fax: 33-32253-4016; E-mail: Michele.tkint@iut.u-picardie.fr.

0008-8846/99/$–see front matter
PII: S0008-8846(98)00232-4

force. Capillary suction depends on both temperature and water content. Capillary suction ceases once the state of full saturation has been reached and then significantly increases near the hygroscopic range.

Wood-clay-cement composites are materials exhibiting a double porosity, whereby the mesoporosity is essentially localised in the clay-cement matrix [10]. The macroporosity results from the wood aggregates. The purpose of the work herein is to determine the influence of this increase in macroporosity that is due to the wood aggregates on the hydric exchanges in either the vapour stage or the liquid phase under classical temperature conditions, i.e., 20°C.

1. Experimental set-up

l.1. Materials

The clayey fines used in this work are almost exclusively composed of kaolinites. Their absolute density, as measured by water pycnometry, is 2.65 g/cm^3, and the Atterberg limits reveal that the clayey material is somewhat malleable [11]. The cement used is CPA CEM I 52.5 (EN 196-1). The aggregates are commercialised Picea wood aggregates of between 3 and 8 mm which have undergone both thermal and physical-chemical treatments. These treatment procedures do not affect the macroporosity of the wood aggregates (see Fig. 1). A more detailed description of the materials is given in reference [10].

1.2. Sorption-desorption measurements

In this work, the sorption-desorption isotherms have been obtained by placing samples with dimensions of 100 × 50 × 25 mm into a Heraeus climatic cell with nine different levels of relative humidity. Three specimens from each mix were used. Two series of samples have been generated. The first series is composed of dry samples. The samples of the second series had been saturated beforehand under vacuum. The mean atmospheric temperature is 23 ± 0.5°C. The changes in the water content of the samples is measured by weighing with a scale that is accurate to the nearest mg. The samples are weighed every other day. The testing equilibrium was established by stabilising the mass of the sample for a sufficiently long period of time. The equilibrium time is approximately 10 days for each of the compositions.

1.3. Gamma-ray spectrometer

The layout of the CSTB gamma-ray spectrometer used for determining the water profiles at certain times intervals is shown schematically in Fig. 2. The equipment consists of three main parts: (a) the radioactive source, 241 Americium with an energy of 60 keV; (b) the detector and the analyser, which form the most important part of the gamma-spectrometer; (c) the gamma-spectrometer, which is interfaced with a computer that controls and synchronises the movement of the source detector assembly and the movement of the sample. Programs are available for data acquisition, data processing, display, and printing [12]. The dimensions of the samples are 4 × 4 × 16 cm. At first, the sample is dried at 70°C after a cure of 28 days in the casting room. Then, it is embedded in a watertight coating made with an epoxy resin. Finally, the studied sample is brought into contact with water and the scanning can be carried out at different time and heights of the measurement.

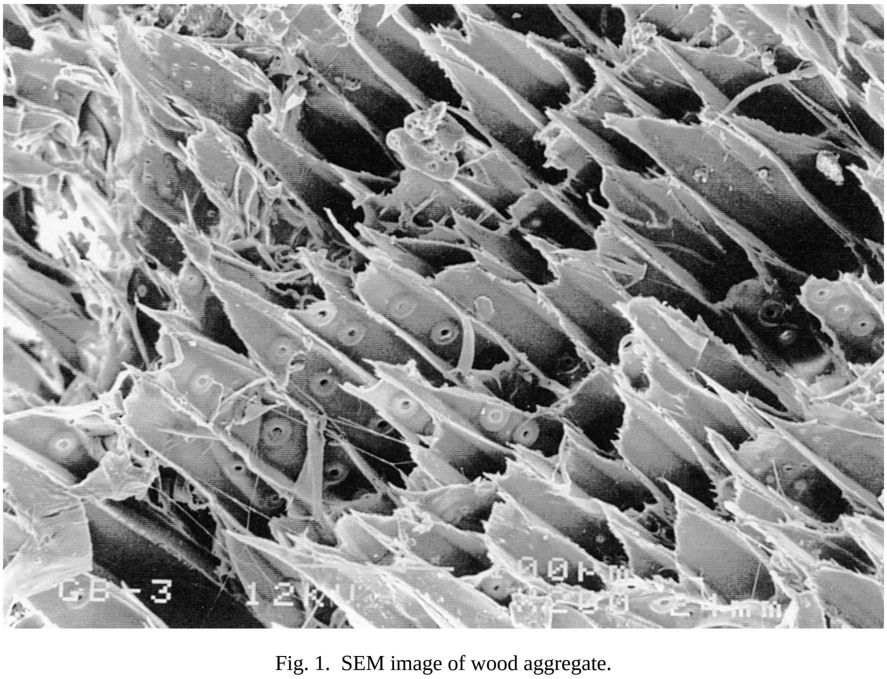

Fig. 1. SEM image of wood aggregate.

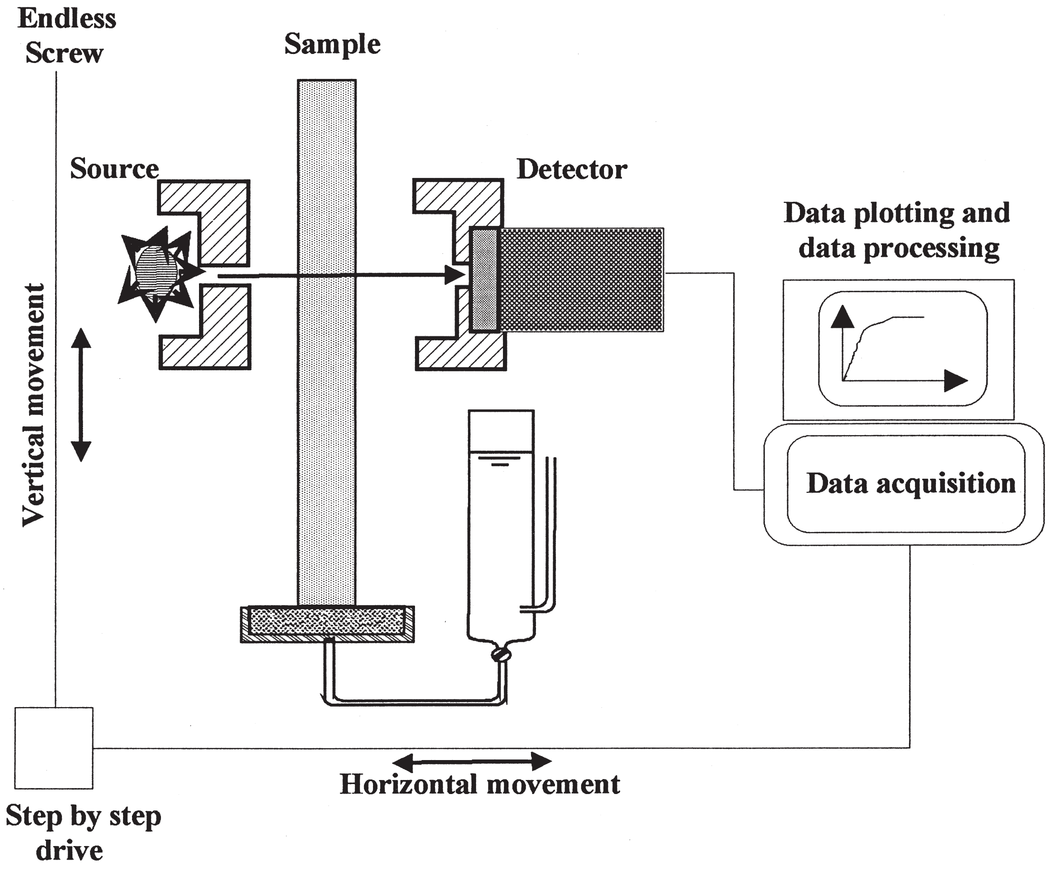

Fig. 2. CSTB gamma-ray spectrometer.

1.4. Magnetic resonance imaging (MRI)

All experiments were performed on a 4.7 Tesla/40 cm Bruker Biospec imager equipped with 152 mm inner diameter (38G/cm) gradient coil system. The transmitter-receiver coil (inner diameter 70 mm) was of the bird cage type. The acquisition sequence is a simple spin echo with short echo time (2 ms). The slice thickness is 1 mm and the resolution 0.275 mm in each direction (256 × 256 image). Two samples with dimensions 5 × 5 × 5 cm were prepared and dried to constant mass at 70°C. After weighing, the first sample has been water impregnated under vacuum, and the second by capillarity by immersion for 48 h in 3 mm of water on one of its sides in a covered tank. The water impregnations were made at a constant temperature of 20°C. Then, the samples were weighed and embedded in a watertight coating and placed in the MRI cell for measurement.

2. Experimental results and analysis

2.1. Sorption-desorption isotherms

Fig. 3 shows all of the sorption-desorption isotherm curves. These curves form a hysteresis. The experimental values were derived as the mean of three independent measurements conducted on each sample. The relation mass water content (w) and the relative humidity (ϕ), denoted w(ϕ) is in fact not independent, but rather depends on the changes in the relative humidity. This phenomenon was analysed by Everett [13], who provides an explanation for this behaviour. The first reason herein pertains to the difference in curvature radii of the fluid-vapour interface, which is assumed to be cylindrical during sorption and spherical during desorption inasmuch as the curvature radius of a spherical surface is half that of a cylindrical surface with the same radius. Based on this fact, Kelvin's Law shows that for a single value of relative humidity, two different values of water content at equilibrium are indeed possible. The second reason lies in the presence of ink-bottle effects which result from the interconnection of pores of different sections. The curves were smoothed using the Hilleborg model, which has already been validated in the case of autoclaved aerated cellular concrete [14]. This model effectively reconstructs the speed of the sorption isotherm but adapts less well to the case of desorption due to the hysteresis phenomenon. We can also note that a small amount of water is taken back into the composite at between 0 and 76% relative atmospheric humidity. Beyond this threshold value, the increase in water content is very significant. When ϕ is 99.9%, the equilibrium water content of the clay-cement

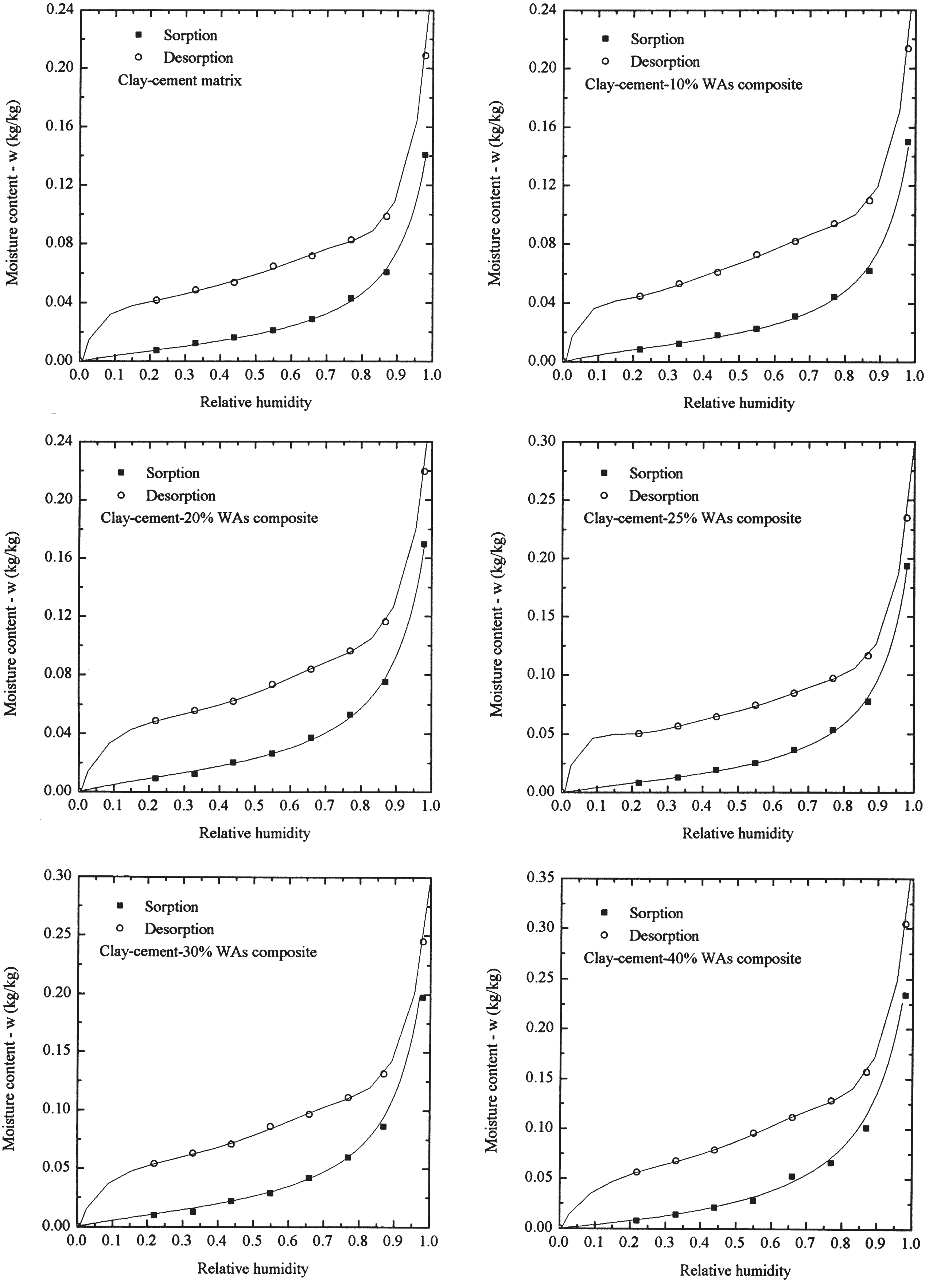

Fig. 3. Sorption-desorption isotherms of various mixtures obtained by substituting clay with wood aggregates.

Table 1
Physical properties of materials

Relative mass percentage of wood aggregates $W_{A_s}/(W_{A_s} + Cl)$*	Dry bulk density (g cm^{-3})	Total porosity (vol. %)	Specific surface area of pores (m^2/g)
0	1.283	48.5	26.98
10	1.065	54.6	28.09
20	0.904	62.1	34.09
25	0.862	63.6	39.03
30	0.800	64.9	34.15
40	0.681	67.7	40.25

* W_{As}: wood aggregates; Cl: clay.

matrix is high in comparison with that at saturation (total porosity, see Table 1), which suggests that the material does exhibit a hygroscopic behaviour. This phenomenon has already been remarked for the case of cement mortar [14]. As regards the clay-cement-wood composite and ignoring the wood content, the water content at equilibrium when ϕ is approximately 99.9% is much less than the water content at saturation under vacuum. This finding can be linked to the increase in macroporosity due to the rising percentage of wood aggregates. The mass of water being absorbed in the macropores results from pure adsorption over almost all of the field; capillary condensation in these macropores does not start until the values of ϕ are very close to 100%.

Finally, the strong hysteresis which affects the sorption isotherms spreads out for low ϕ values. It should be pointed out that hysteresis only affects capillary condensation and that for small values of ϕ, only surface adsorption is actually affected. Given the complexity of this phenomenon, the explanation forwarded herein is that certain micropores exist which are undetectable by mercury porosimetry, whereby the strong affinity for water can result in a high retention of water in desorption. This phenomenon has already been noted in the case of wood [15].

2.2. Water absorption

The moisture profiles measured during the absorption of water in a clay-cement matrix and in a composite containing 30% wood aggregates are shown in Figs. 4 and 5. The application of the Boltzmann transformation serves to combine the various measured moisture profiles that correspond to the different positions into a single profile: see Figs. 6 and 7. Note that the values of the water content measured around the origin, which corresponds to the capillary moisture content, are much less than those of the composite ($\theta_v = 30\%$, whereas the total measured porosity is $\varepsilon = 65\%$). It follows then that in the presence of air, a large portion of the porous volume is not involved in the wetting process. The incomplete saturation by capillarity in the case of the clay-cement composite with a 30% wood content can also be confirmed by determining the capillary suction. This step was carried out both by using the isotherm sorption curves and Kelvin's law in the hygroscopic domain and by using mercury porosity from Mualem's model in the capillary domain [16–18]. We can observe in Fig. 8 that the limit of the column's water content is of the same order of magnitude as that which had been determined experimentally. The difference was qualitatively confirmed using standard magnetic resonance imaging techniques on two samples of the same material (25% wood content), one saturated under vacuum and the other by capillarity (see Figs. 9 and 10). Note that in these MRI images, the water contents differ depending on the saturation process. Measuring the volumic contents in water lead to values of approximately 61.3% in the case of saturation under vacuum, and 44% in the case of saturation by capillarity. In addition, this water gets divided differently depending on the saturation mode. In the case of saturation by capillarity, water essentially diffuses inside a clay-cement matrix and remains in the small pores. Indeed, the MRI method shows only a few coloured stains, thereby demonstrating an accumulation of water while the mass content of water is 55%, i.e., more than half of the mass of the sample.

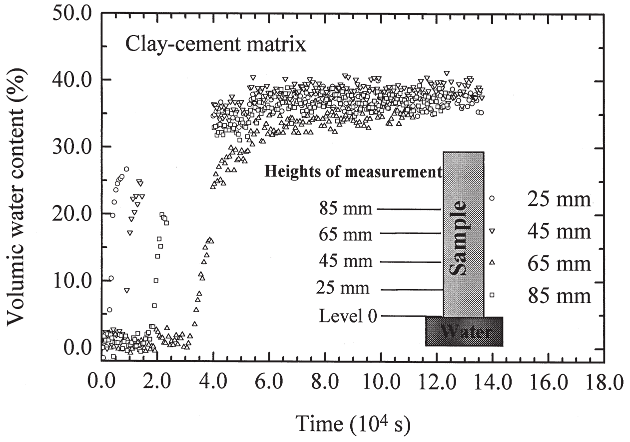

Fig. 4. Moisture profiles measured during the absorption water in a clay-cement matrix at isothermal conditions.

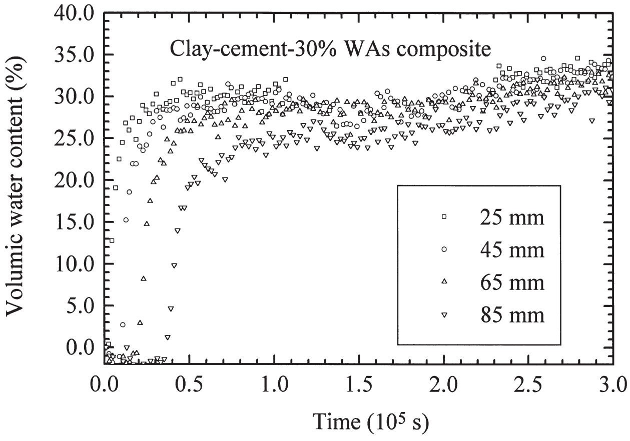

Fig. 5. Moisture profiles measured during the absorption water in a clay-cement-30% wood aggregates composite at isothermal conditions.

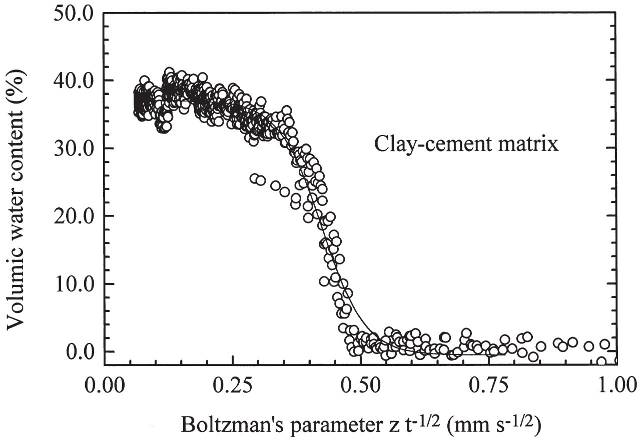

Fig. 6. Boltzmann transformation of the measured moisture profiles for the clay-cement matrix.

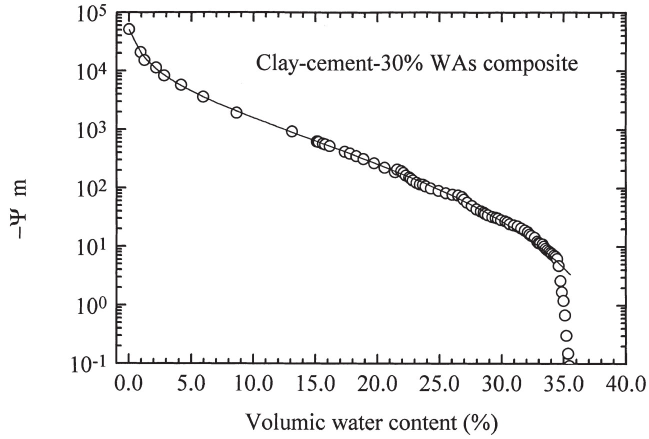

Fig. 8. Capillary suction curve of the clay-cement-30% wood aggregates composite obtained by using Kelvin's law in the hygroscopic domain and by using Mualem's model in the capillary domain.

It is well known that MRI imaging does not enable detecting a pore diameter of less than 1 μm. In order for a molecule of water to be detectable, it must be able to vibrate under the impulsion of a magnetic field. It is also well known that water molecules are adsorbed by the pore's walls when in close contact. Should the size of the pore filled with water be large, this effect would be negligible. As the pore size decreases, the percentage of water molecules adsorbed, in comparison with the total water volume, rises. Not detecting any water through the use of the MRI technique does not necessarily signify an absence of water in the sample. Consideration must also be given to the measured mass content of water. In the case of saturation under vacuum (see Fig. 9), the differential accumulation and the filling of the larger-sized pores can be easily distinguished in the matrix. This phenomenon can be explained by the presence of the macropores, which are basically due to the macrostructure of wood aggregates embedded in a clay-cement matrix that contains essentially the micropores. These macropores tend to slow down significantly the movement of the thin trickles inside the material. It has also been shown [19] that the average propagation speed of capillary meniscus can be considerably greater in homogeneous and small-ray circuits than in the case of systems containing interconnected sections with larger rays. The capillary invasion can therefore occur mainly through small-ray homogeneous canals that serve to prevent the filling of larger-sized pores. This phenomenon has also been confirmed by the microstructural analysis based on the pore-size distributions [10]. In a clay-cement matrix, only 5% of the pores with diameters greater than 1 μm are observed, in comparison with 85% in wood aggregates. The composite contains 25% of wood aggregates and 35% of pores. In addition, the curve of the mercury porosimetry withdrawal reveals that a significant portion is not restored (only 44% for a composite of 30% aggregates). This finding confirms both the interconnection of pores with various diameters and the presence of "ink-bottle effect" pores. Moreover, the nonsorption effect of wood aggregates on the capillary absorption of the composite can be observed. This effect has already been identified for other types of construction materials, as presented in the Hall et al. [20] study of plasters and other nonsorptive filler mortars. This phenomenon of sorptivity [21–28], changes a material's capacity to absorb water by capillarity for certain initial conditions as well as for given limits. The calculation of the coefficients of sorptivity from the moisture profiles allows us to show that the presence of wood aggregates results in a significant reduction in the sorptivity, with 1.55 and 0.97 mm/min$^{1/2}$ representing 0 and 30% of wood aggregates, respectively.

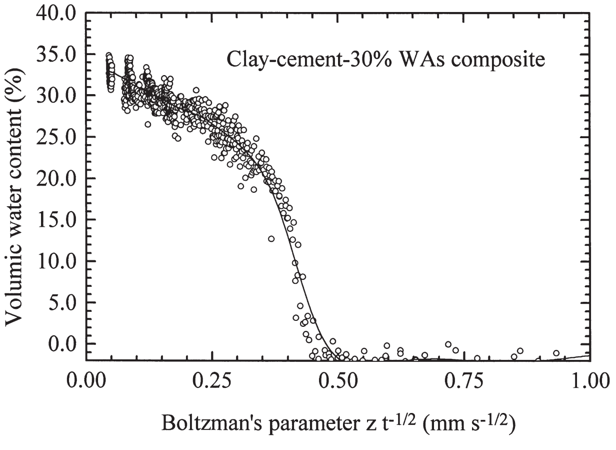

Fig. 7. Boltzmann transformation of the measured moisture profiles for the clay-cement-30% wood aggregates composite.

Finally, the total moisture diffusivity is represented in Fig. 11. Its value could not be determined for small water content values, due to the difficulty in measuring the diffusivity of the vapour stage. For small values of water contents, the condensation phase is in fact either in an absorbed form or in liquid islands. The transfer to vapour water is the

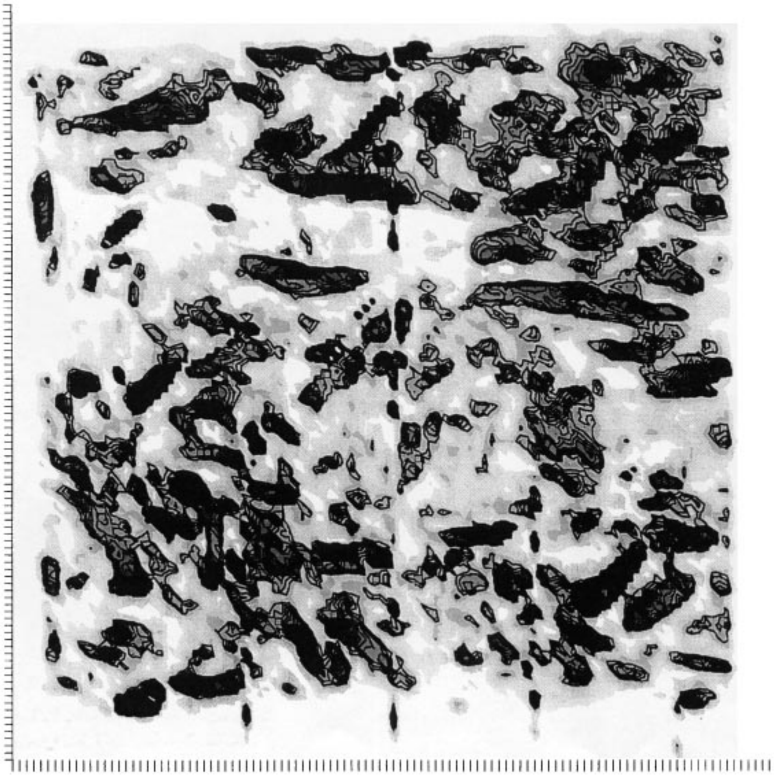

Fig. 9. Magnetic resonance image of clay-cement-25% wood aggregates saturated in a vacuum.

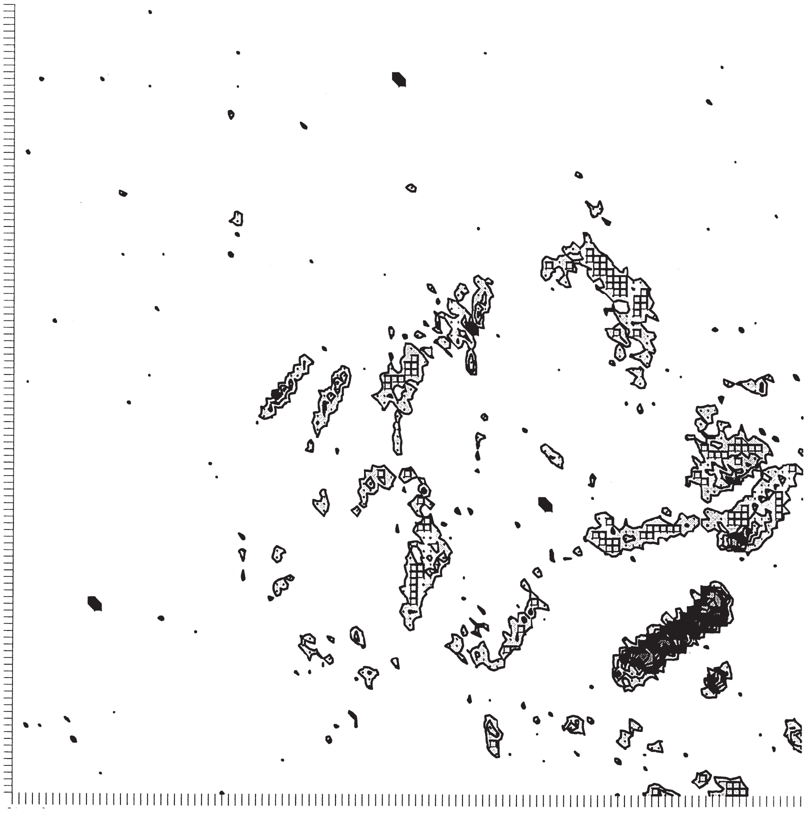

Fig. 10. Magnetic resonance image of clay-cement-25% wood aggregates saturated by capillarity.

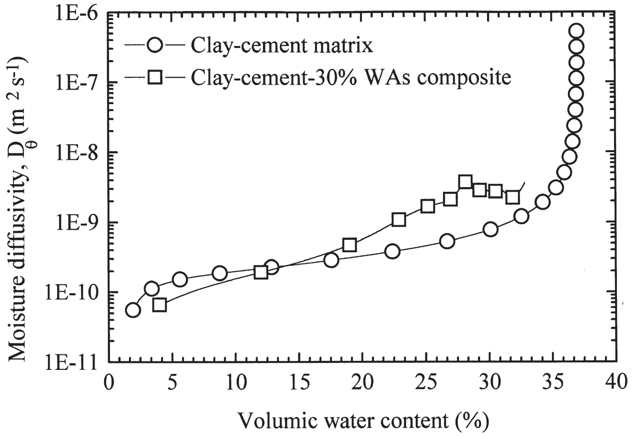

Fig. 11. Moisture diffusivity for clay-cement matrix and clay-cement-30% of wood aggregates composite.

only phenomenon being considered. As the water content increases, a mixed liquid-vapour diffusion appears. The transfer to the liquid phase dominates at high values of water content.

Experimental results show that the moisture diffusivity D_θ changes with the water content of the sample. We can also highlight that for a volumic water content between 0 and 15%, i.e., the hygroscopic domain, the moisture diffusivity of the composite is less than that of the clay-cement matrix. It thus seems that the wood aggregates block the diffusion of the vapour. The gamma-ray attenuation method does not distinguish between water in both the vapour and liquid stages. Beyond a volumic water content of 15%, the wood aggregates do not seem to participate to the liquid phase transfer because of their macroporous structure. Thus, the liquid transfer occurs mainly in the microporous clay-cement matrix.

In the case of a clay-cement matrix, the transfer to the liquid phase dominates at high water content values. Nevertheless, this phenomenon has not been observed in the case of composites, as the total saturation was not reached by capillarity.

3. Conclusions

Hilleborg's model based on the model adsorption theory was used for fitting the sorption isotherms. It is found that this model effectively reconstructs the speed of the sorption isotherms for adsorption, but failed for the desorption, due to the entrapment of air and other effects for all mixtures. Although the hysteresis only affects capillary condensation, it is also shown that the sorption isotherms present a strong hysteresis for law relative humidity values.

The gamma-ray spectrometer turns out to be an effective tool to investigate nonsteady moisture transfer through wood cementitious composites.

The results of Mercury Porosimetry Intrusion can be used to estimate the capillary suction as a function of water content, which is an important parameter. Consequently, much experimental work could be avoided.

From MRI measurements, it has been demonstrated that upon contact with liquid water, the presence of wood aggregates leads to both slowing down the progression of capillary wetting and decreasing the quantity of water being absorbed by the material. The water migration has been found to occur in microporous matrix. Moreover, the absorption of water in the vapour phase remains relatively weak with regard to the one absorbed by capillary wetting.

Generally, the moisture diffusivity increases rapidly with increasing the volumic water contents. Furthermore, it is found that in the hygroscopic domain, the wood aggregates block the diffusion of the vapour within the material. This phenomenon persists up to a critical value of volumic water content, θ_{vc}, which corresponds to the limit between the hygroscopic domain and capillary domain. So, for volumetric water content greater than θ_{vc}, the wood aggregates' contribution to the liquid phase transfer becomes negligible because of their nonsorptive character.

It is worth mentioning that although the results obtained from gamma-ray spectrometer concern only the clay-cement matrix and the clay-cement-30% wood aggregates composite, the role of wood aggregates in the capillary absorption of wood cementitious composite has been confirmed from thermal conductivity measurements and their dependence on temperature and moisture contents for all mixtures.

References

[1] F.J. Hogan, J.W. Meusel, Cem Concr Aggregate 3 (1981) 40.
[2] X. Wu, D.M. Roy, Cem Conc Res 14 (1984) 521.
[3] D.A. Rose, Br J Appl Physics 14 (1963) 256.
[4] A. Hillerborg, Cem Conc Res 15 (1985) 809.
[5] I. Langmuir, J Am Chem Soc 38 (1985) 2221.
[6] I. Langmuir, J Am Chem Soc 40 (1918) 1361.
[7] S. Brunauer, P.H. Emmett, E. Teller, J Am Chem Soc 60 (1938) 309.
[8] M. Douglas, Principles of Adsorption and Adsorption Processes, John Wiley & Sons, New York, NY, 1984.
[9] R.F. Feldman, Yi Huang Cheng, Cem Concr Res 15 (1985) 765.
[10] A. Bouguerra, A. Ledhem, F. De Barquin, R.M. Dheilly, M. Queneudec, Cem Conc Res 28 (1998) 1179.
[11] K. Al Rim, A. Ledhem, M. Queneudec, Mat and Struct 29 (1996) 514.
[12] D. Quénard, H. Sallée, Proceedings of Symposium on Pore Structure and Permeability of Cementitious Materials, Boston, USA, 1988.
[13] D.H. Everett, J.M. Haynes, J Colloid and Interface Sci 38 (1972) 125.
[14] D. Quénard, Adsorption et transfert d'humidité daus les matériaux hygroscopiques: approche du type percolation et expérimentation, PhD Thesis, INP Toulouse, 1989.
[15] C. Skaar, Proceedings of Symposium on Wood Temperature and Humidity Relationships, Blacksburg, Madison, WI 1979, p. 23.
[16] Y. Mualem, Water Resources Res 10 (1974) 514.
[17] Y. Mualem, G. Dagan, Water Resources Res 11 (1975) 452.
[18] Y. Mualem, Soil Sci 13 (1984) 283.
[19] F.A.L. Dullien, Porous Media: Fluid Transport and Pore Structure, Academic Press, New York, NY, 1979.

[20] C. Hall, W.D. Hoff, M.A. Wilson, J Physics D. Appl Physics 26 (1993) 31.
[21] R.J. Gummerson, C. Hall, W.D. Hoff, Construct Papers 1 (1980) 17.
[22] C. Hall, W.D. Hoff, M. Skeldon, J Physics D. Appl Physics 16 (1983) 1875.
[23] C. Hall, W.D. Hoff, Building and Environ 21 (1986) 113.
[24] C. Hall, Mag Conc Res 41 (1989) 51.
[25] M.A. Wilson, W.D. Hoff, C. Hall, Building and Environ 29 (1994) 99.
[26] M.A. Wilson, W.D. Hoff, Building and Environ 29 (1994) 537.
[27] C. Hall, Mat and Struct 27 (1994) 291.
[28] C. Hall, K. Green, W.D. Hoff, M.A. Wilson, J Physics D. Appl Physics 29 (1996) 2947.